ISSN 1009-3095 *Journal of Zhejiang University(SCIENCE)* V.1, No.2, P.129-135, Apr.-Jun., 2000
http://www.zju.edu.cn; http://www.zjupress.com; http://www.chinainfo.gov.cn/periodical

NUMERICAL INVESTIGATION ON THE PHASE CHANGE OF WATER-SATURATED POROUS MEDIA WITH THERMOSYPHON

WU Cun-zhen(吴存真)[1], PAN Yang(潘阳)[2], QIN Yue-hui (秦悦慧)[1]

([1]*Dept. of Energy Engineering, Yuquan Campus of Zhejiang University, Hangzhou, 310027, China*)
([2]*Dept. of Civil Engineering, East China Jiaotong University, Nanchang, 330013, China*)

Received Dec.12, 1998; revision accepted May.18, 1999

Abstract: Numerical investigations were carried out to determine the coupled heat transfer of water-saturated porous media with a two-phase closed thermosyphon for soil freezing, and to examine the characteristics of the freezing heat transfer in the water-saturated porous media. The whole control volume includes the thermosyphon and the porous media. The two-dimensional governing equations for the water-saturated porous media are used.

The conjugation of heat transfer between the thermosyphon and porous media is reflected through thermal balance between the thermosyphon and the porous media.

The finite-difference method was used to solve the two-dimensional governing equation for the water-saturated porous media and the heat transfer characteristics of the thermosyphon, obtain the flow fields and the temperature distributions in the soil. This paper deals mainly with the effect of some factors (such as soil properties, climate and thermosyphon dimensions) on the heat transfer rate of the thermosyphon and the growth of the freezing front. The predictions of the present study agree well with the measured data.

Key words: thermosyphon, water-saturated porous, soil freezing, coupled heat transfer
Document code: A **CLC number:** TK214

INTRODUCTION

In cold regions, soil expansion resulted from a soil freezing process often deforms and damages some construction foundations. One way to stabilize the foundation is use of two-phase closed thermosyphon in the cold regions. Due to its excellent heat transfer characteristics, the two-phase closed thermosyphon placed in the soil can change the soil temperature distributions and the water-saturated flow field, thicken the freezing front, and limit soil expansion.

Freezing heat transfer in water-saturated porous media was extensively investigated (Beckermann, 1988; Sasaki et al, 1989; 1990). The transient conjugate heat transfer of the thermosyphon with freezing of pure water was investigated experimentally and numerically by Wu and Gu (1989; 1993). However, there are no reports of study on the coupled heat transfer of a vertical two-phase closed thermosyphon with the soil, and on the water-saturated soil freezing resulted from the coupled heat transfer.

Based on the governing equations for the porous media(soil) and the heat transfer characteristics of the thermosyphon, the present work is aimed to derive a numerical model to describe the coupled heat transfer of a vertical two-phase closed thermosyphon with water-saturated soil freezing; and is focused on the effect of the soil properties, the climate conditions and the thermosyphon characteristics on the coupled heat transfer and the soil freezing processes. This numerical model outputted predictions agreeing well with measured data and can be used to predict soil temperature distribution and soil freezing processes, and direct engineering applications of the thermosyphon for cold regions.

ANALYSIS

The physical model established in this study is a two-dimensional cylinder coordinate system as depicted in Fig.1.

The heat flux in the soil is transferred and dissipated into the environment by a two-phase closed thermosyphon, with its evaporator Le is placed in the water-saturated porous media(soil) and its condenser Lc opened to the air. The initial temperature of the porous media is above its freezing point. When the air temperature is be-

low the soil temperature, the condenser of the thermosyphon is cooled by the chill air, and the thermosyphon begins to work. The heat flux of the thermosyphon is influenced by the soil heat transfer, while the change of the soil temperature distribution and the freezing layer thickness are controlled by the heat flux of the thermosyphon. This process is a coupled heat transfer between the thermosyphon and the soil freezing.

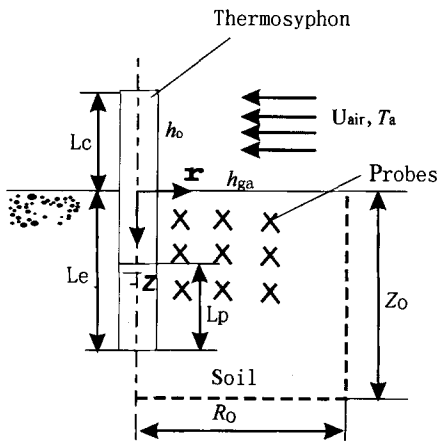

Fig. 1 Schematic diagram

For the soil, the following assumptions are made:

(1) The soil is a porous medium with isotropic and homogeneous properties,

(2) The fluid flow in the unfrozen porous layer is laminar and incompressible,

(3) Volume change resulted from the freezing expansion can be negligible and the particles of the porous medium are rigid,

(4) Thermophysical properties of the water are constant except for its density.

Under these assumptions, the governing equations are as follows.

In the porous media, the continuity, momentum, and energy equations are

$$\frac{\partial(ru)}{\partial z} + \frac{\partial(rv)}{\partial r} = 0 \tag{1}$$

$$\left(\frac{\rho_l}{\varepsilon}\right)\frac{\partial u}{\partial \tau} + \left(\frac{\rho_l}{\varepsilon^2}\right)\left(u\frac{\partial u}{\partial z} + v\frac{\partial u}{\partial r}\right) = -\frac{\partial p}{\partial z} + \left(\frac{\mu_l}{\varepsilon}\right)\left(\frac{\partial^2 u}{\partial z^2} + \frac{\partial^2 u}{\partial r^2}\right) - \left(A + \frac{\mu_L}{K} + \frac{\rho_L C \mid u \mid}{K}\right)u - \rho_m g\Omega \cdot (\mid T_f - T_m \mid^q - \mid T - T_m \mid^q) \tag{2}$$

where the values of T_m, ρ_m, Ω and q in Eq. 2 were taken from Gebhart and Mollendort (1977).

$$\left(\frac{\rho_l}{\varepsilon}\right)\frac{\partial u}{\partial \tau} + \left(\frac{\rho_l}{\varepsilon^2}\right)\left(u\frac{\partial v}{\partial z} + v\frac{\partial v}{\partial r}\right) = -\frac{\partial p}{\partial z} + \left(\frac{\mu_l}{\varepsilon}\right)\left(\frac{\partial v^2}{\partial z^2} + \frac{\partial v}{\partial r^2}\right) - \left(A + \frac{\mu_L}{K} + \frac{\rho_L C \mid v \mid}{K}\right)v \tag{3}$$

$$\rho c\frac{\partial T}{\partial \tau} + \rho c_l\left(u\frac{\partial T}{\partial z} + v\frac{\partial T}{\partial r}\right) = k_{\text{eff}}\left(\frac{\partial^2 T}{\partial z^2} + \frac{\partial^2 T}{\partial r^2}\right) + \varepsilon\rho_l\Delta h\frac{\partial f}{\partial \tau} \tag{4}$$

where

$$K = \frac{d^2\varepsilon^2}{150(1-\varepsilon)^2} \tag{5a}$$

$$C = \frac{1.75d}{(150\varepsilon^2)^{0.5}} \tag{5b}$$

$$\rho c = \varepsilon[f\rho c_l + (1-f)\rho_s c_s] + [1-\varepsilon]\rho_p c_p \tag{5c}$$

$$k_{\text{eff}} = \varepsilon[fk_l + (1-f)k_s] + (1-\varepsilon)k_p \tag{5d}$$

where

A constant in Eq. 2 and 3
C defined in Eq. 5a
d particle diameter of porous medium
g gravitational acceleration
Δh latent heat of solidification
K permeability of porous medium
k_l thermal conductivity of liquid
k_s thermal conductivity of solid
k_p thermal conductivity of porous medium
k_{eff} effective conductivity
p pressure
T_f freezing temperature
τ time
ε porosity
v kinematic viscosity
c_p specific heat of porous medium
f local liquid fraction
r radial coordinate
u velocity in z direction
z axial coordinate
ρ_l density of liquid
μ_l dynamic viscosity of liquid

For the thermosyphon, the following assump-

tions may be made:

(1) The liquid film inside the thermosyphon is laminar and the effect of the vapor flow can be negligible;

(2) The vapor in the thermosyphon is saturated and uniform in temperature;

(3) The evaporator section of the thermosyphon consists of two parts: the liquid film and the boiling pool. The temperature of the liquid film equals the vapor temperature. The boiling pool's saturation temperature varies with height due to the hydrostatic pressure.

The heat transfer coefficients for the condensation, film evaporator and boiling pool are written respectively as follows (Shirail, 1982, He and Ma, 1992a, 1992b).

$$h_c \frac{(v_l^2/g)^{1/3}}{k_l} = (4/3)^{4/3} Re_c^{-1/3} \tag{6}$$

where

$$Re_c = \frac{4q_c L_c}{\lambda \mu_1}$$

$$h_f \frac{(v_l^2/g)^{1/3}}{k_l} = (4/3)^{4/3} Re_f(z)^{-1/3} \tag{7}$$

where

$$Re_f(z) = \frac{4q_e(L_e - z)}{\lambda \mu_l}$$

$$\frac{h_p d_i}{k_i} = 14.45\left(\frac{d_i q_e}{\lambda \mu_l}\right)^{0.39} Pr^{0.75}\left(\frac{\rho_l}{\rho_v}\right)^{0.2}\left(\frac{H_p^* Le}{d_i}\right)^{0.12} \tag{8}$$

where the dimensionless boiling pool height is

$$H_p^* = \frac{H_p}{Hl} = (1.59F^{0.95} Re_f^{-0.35} H_l{}^{*0.37} + 1)L_e \tag{9a}$$

$$H_l^* = L_p/L_e \tag{9b}$$

$$F = \frac{4q_e L_e}{\rho_v \lambda}/\{1.53[\sigma g[\rho_l - \rho_v)/\rho^2 v]^{0.25}\}\, d_i \tag{9c}$$

$$Re_f = \frac{4q_e L_e}{\lambda \mu_l} \tag{9d}$$

where

h_c heat transfer coefficient of condensation
h_f heat transfer coefficient of liquid film
h_p heat transfer coefficient of liquid pool
Re_c Reynolds number of condensation
Re_f Reynolds number of liquid film
λ latent heat of vaporization
σ surface tension
v_l kinematic viscosity of liquid
H_p height of liquid pool
H_l height of liquid
H_p^* dimensionless height of liquid pool
H_l^* dimensionless height of liquid
L_p length of liquid pool
L_e length of the evaporator section
l_c length of condensation
q_c heat flux of condensation
q_e heat flux of the evaporator section
Pr Prandtl number
ρ_v density of vapor
d_i inner diameter
k_i inner conductivity

The conjugation of heat transfer between the thermosyphon and porous media is reflected through thermal balance between the thermosyphon and the porous media.

$$k_{\text{eff}} \frac{\partial T}{\partial r}\bigg|_{r=R_i} = h_e(T_s - Tw_e) \tag{10}$$

where

h_e heat transfer coefficient of the evaporator section
T_s temperature of saturated
T_{w_e} wall temperature of east nodal

However, one of the important problems for the coupled heat transfer is to find the wall temperature distribution of the thermosyphon since the wall of the thermosyphon is an interface of the coupled heat transfer and the boundary conditions for the soil heat transfer.

Where

$$T_s(z) = \begin{cases} T_v \text{ for liquid film} \\ f[P(T_v) + \rho_l g(z - L_e + H_p)] \text{ for liquid pool} \end{cases} \tag{11}$$

$$h_e = \begin{cases} h_f & \text{for liquid film} \\ h_p & \text{for liquid pool} \end{cases} \tag{12}$$

The initial and boundary conditions for the entire porous domain are

$$\tau = 0: T = T(z), u = 0, v = 0$$

$$z = 0: k_{\text{eff}} \frac{\partial T}{\partial z} = h_{\text{ga}}(T - T_a), u = 0, v = 0$$

$$z = \infty: T = T(\tau), u = 0$$

$$z > L_c, r = 0: \frac{\partial T}{\partial r} = 0, v = 0$$

$$z \leq L_c, r = R_0: T = Tw_e(z), u = 0, v = 0$$

$$r = \infty: \frac{\partial T}{\partial r} = 0, v = 0$$

where h_{ga} is the heat transfer coefficient between ground surface and air.

THE METHODOLOGY

A general form can be obtained for the governing equations from Eqs. 1 through 4

$$B_1 \frac{\partial \Phi}{\partial \tau} + B_2 \nabla \cdot (V\Phi) = \nabla \cdot (B_3 \nabla \Phi) + S \tag{13}$$

Where Φ is a general dependent variable, V is the velocity factor. The values from B_1 through B_3 are the coefficients of the relevant equations. These equations are discretized with the control volume based on the finite-difference formulation and solved by the SIMPLE algorithm (Patankar et al., 1980).

In the energy conservation equation, the local liquid fraction of this time step in each control volume must be updated by that of the last time step(Lacroix et al., 1990).

$$f = f^0 + (\sum a_{hb} T_{nb} + a_p^0 T_p^0 - a_p T_p)[\varepsilon c_l \Delta\tau / (\rho_l \Delta h \Delta V)] \tag{14}$$

where a_{nb} and T_{nb} are coefficients and temperature of the near nodes, respectively. $a_p^0 T_p^0$ and $a_p T_p$ are the old values and present values of the node, respectively.

If $f < 0$ then set $f = 0$

If $f > 1$ then set $f = 1$

If $0 < f < 1$ then set $T = T$

Calculations begin from the thermosyphon in the present study. At first, according to Eqs. 5 to 13, the wall temperature of the evaporator of the thermosyphon is evaluated from the heat rate transferred by the thermosyphon which is assumed or calculated at the last time step. Next, in the light of the boundary conditions and the wall temperature of the evaporator, the temperature field and the stream function are obtained by Eqs. 1 to 3. And the heat rate of the thermosyphon is renewed. Then the iterations are repeated until the following criterion is satisfied at all the grid points:

$$\left| \frac{Q_r - Q_b}{Q_r} \right| < 10^{-3} \tag{15}$$

Where

$$Q_r = \int_0^{z_0} \int_0^{R_0} [\rho c(T - T^0) + \varepsilon \rho \Delta h \cdot (f - f^0)] r dr dz$$

$$Q_b = Q_w + Q_e + Q_s + Q_n$$

Eq. 16 is the error range of the energy balance equation. Q_r denotes the enthalpy increase of the control volume caused by temperature, local liquid fraction and phase change. Q_w, Q_e, Q_s and Q_n denotes the energy transferred through the west, east, south and north nodal, respectively. Q_b denotes the total energy transferred through all boundary surfaces. Q_r must equal Q_b, which is the energy balance equation.

RESULTS AND DISCUSSIONS

In this paper, the values of some parameters, such as porosity of soil(ε), air temperature(T_a), air velocity(U_{air}) and coefficient (h_{ga}) of heat transfer between ground surface and air that considered the effect of solar radiation are those of the cold region of northeast China. The effect of ε, T_a and the diameter of the thermosyphon (d_0) on heat transfer of the entire domain is considered. Some numerical results, such as streamline, isotherm and freezing front are analyzed. Fig. 2 compares predicted and measured temperature variation with time for the local point under the soil. Each radial point temperature and the temperature variation with time at the same depth of the soil(z) are different under the action of the thermosyphon. The change of temperature for some points near the thermosyphon is more rapid. Fig. 3 shows the predicted and measured change of the freezing front with time. Fig. 2 and Fig. 3 show good agreement between modeled results and experimental data.

The soil porosity ε and the environment air temperature T_a have relevant effect on the heat transfer rate of the thermosyphon and the freez-

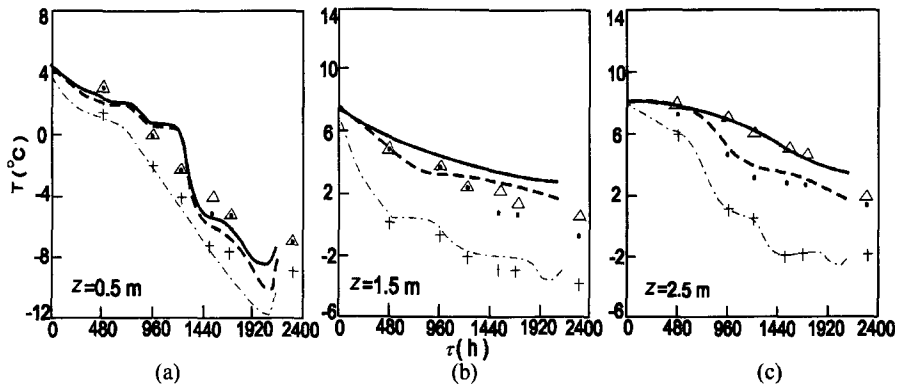

Fig.2 Variation of local soil temperature with time

(a) $z=0.5$m; (b) $z=1.5$m; (c) $z=2.5$m

Radius	$r=0.25$ m	$r=0.75$ m	$r=1.2$ m
Predicted	—·—	— — —	———
Measured	+	·	△

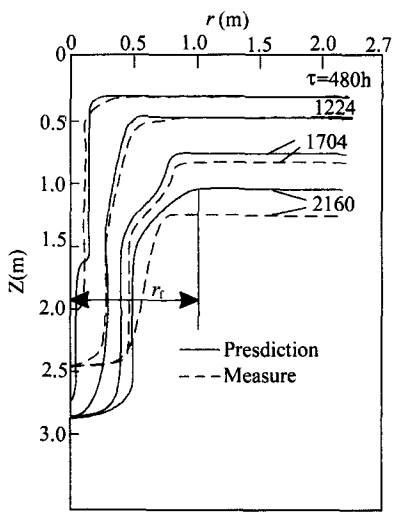

Fig.3 Change of the freezing front with time

ing, respectively, as shown in Fig.4. Obviously, the lower the air temperature, the higher is the heat transfer rate of the thermosyphon, since the temperature difference between the air and the condenser of the thermosyphon is increased. According to the average air temperature of four months in the winter season and air temperature variation of each day in the cold region, T_a is treated linearly. The heat transfer rate of the thermosyphon increases with increase of soil porosity ε, but the frozen region of lower soil porosity is larger than the frozen region of higher porosity (Fig.4). For lower porosity soil, the water content in the soil is less, the freezing scope is wider at the same heat transfer rate. The diameter (d_0) of the thermosyphon affects the heat transfer rate and the freezing front (Fig.5). The rate

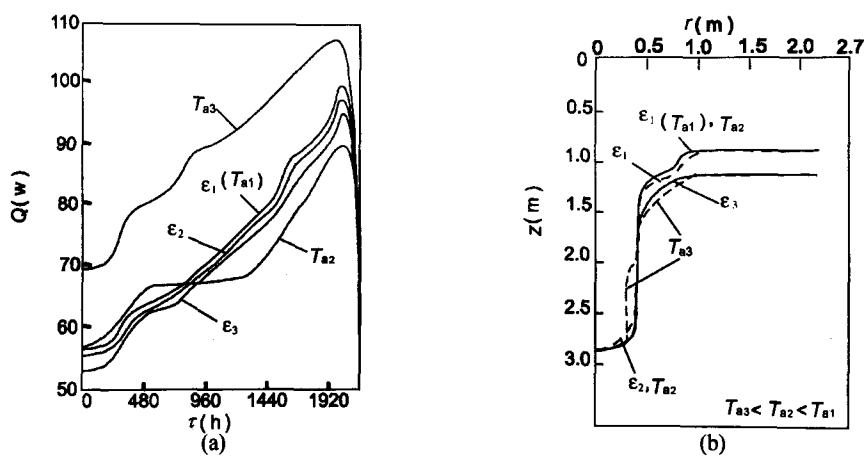

Fig.4 Numerical results for $\varepsilon_1=0.511, \varepsilon_2=0.5, \varepsilon_3=0.48$ and different T_a

(a) heat transfer; (b) freezing front

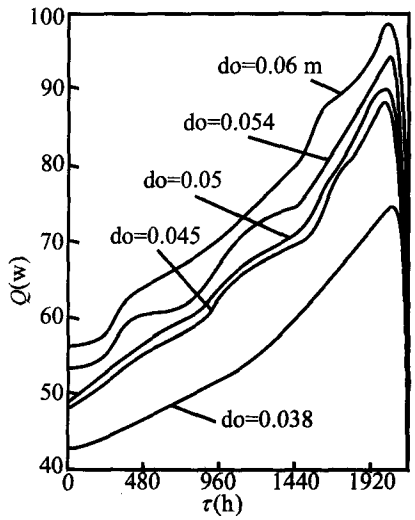

Fig.5 Variation of heat transfer rate with time for different thermosyphon diameters

of the heat transfer inside the thermosyphon increases with increase of thermosyphon diameter.

For the case of $\varepsilon = 0.511$, $d_0 = 0.06$ m, $U_{air} = 2.98$ m/s, $h_{ga} = 8.5$ w/m$^2 \cdot$℃, and air temperature T_a, the patterns of streamlines and isotherms at $\tau = 10$ days are as shown in Fig.6a and 6b, respectively. In Fig.6a, there are two counterrotating vortices due to the density inversion of water near 4 ℃. One of the vortices is the counterclockwise vortex in the <4 ℃ region and near the evaporator of the thermosyphon, and the other is the clockwise vortex in the higher temperature unfrozen region with larger area. With the increase of heat rate transferred from the soil, the freezing region is increased more and more, and the counterclockwise vortex is also increased, as depicted in Fig.7, showing that

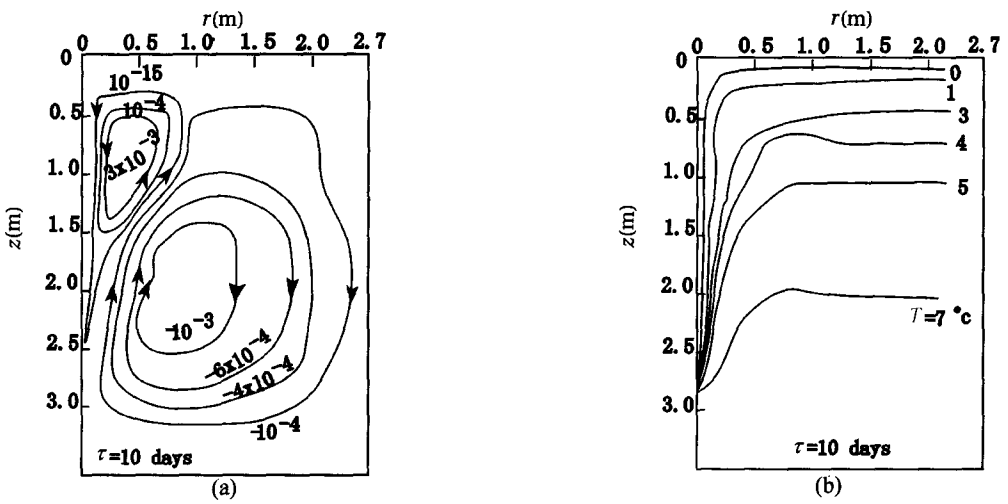

Fig.6 Numerical results for $\tau = 10$ days
(a) streamlines; (b) isotherms

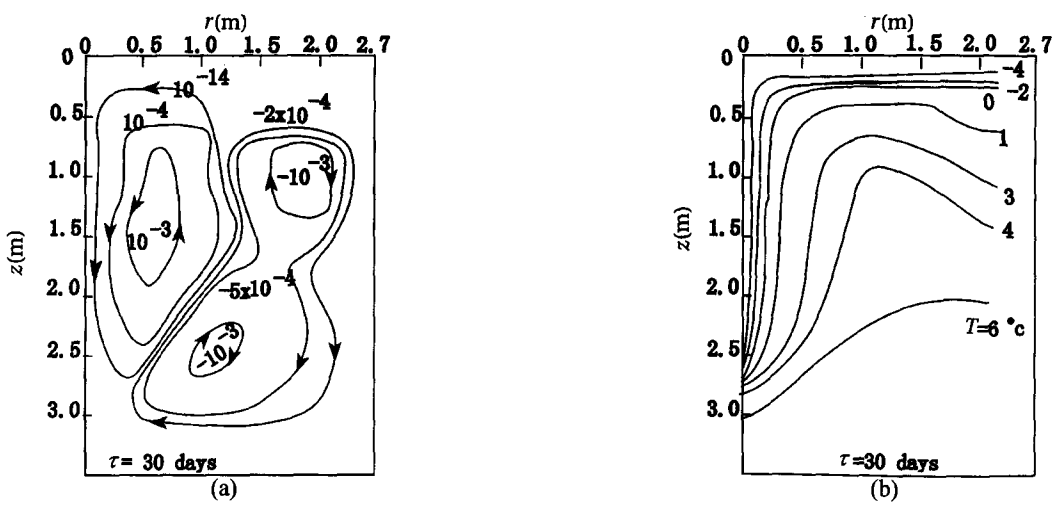

Fig.7 Numerical results for $\tau = 30$ days
(a) streamlines; (b) isotherms

there are two vortices of equal magnitude in the unfrozen region because the density inversion of water near 4 ℃ causes the change of the buoyancy force which divides the >4 ℃ vortex region and the <4 ℃ region.

CONCLUSIONS

A vertical two-phase closed thermosyphon was used in this study on water-saturated soil freezing yielding numerical results agreeing well with experimental data and indicating that the thermosyphon could change the temperature distribution of the soil and the thickness of the freezing front. The heat transfer rate of the thermosyphon is affected by soil porosity, environment temperature and thermosyphon diameter.

References

Beckermann C. and Viskanta R. 1988, Natural convection solid/liquid phase change in porous media. *Int. J. Heat Transfer*, **31**:33 - 46.

Gebhart B. and Mollendort J., 1977, A new density relation for pure and saline water. *Deep Sea Res.*, **24**:831 - 848.

He Jialun, Ma Tongze and Zhang Zhengfang, 1992a, Heat Transfer Characteristics in the Evaporator Section of a Two-phase Closed Thermosyphon, *In*: Advances in Heat Pipe Science and Technology, edited by Ma Tongze. Printing House of China Building Industry Press, Beijing, China, p.335 - 340

He Jialun, Ma Tongze and Zhang Zhengfang, 1992b, Investigation of Boiling Liquid Pool Height of a Two-phase Closed Thermosyphon, *In*: Advances in Heat Pipe Science and Technology, edited by Ma Tongze. Printing House of China Building Industry Press, Beijing, China, p.154 - 159

Lacroix M. and Voller V.R., 1990, Finite difference solution of solidification phase change problem: Transformed versus fixed grids. *Numerical Heat Transfer, Part B*, **17**:25 - 41.

Patankar S. V., 1980, Numerical Heat Transfer and Fluid Flow. Hemisphere Publishing Corporation, Washington D.C., p.1 - 183

Sasaki A., Aiba S. and Fucusako S., 1989a, Transient Freezing Heat Transfer in a Water Saturated Porous Media. Proc. of 2nd Int. Symp. on Cold Regions Heat Transfer, p.291 - 296.

Sasaki A., Aiba S. and Fucusako S., 1990b, Numerical study on freezing heat transfer in water-saturated porous media. *Numerical Heat Transfer, Part A*, **18**: 17 - 32

Shiraish M., Kikuchi. and Yamanish T., 1982, Investigation of Heat Transfer Characteristics of a Two-phase Closed Thermosyphon, Advances in Heat Pipe Technology. Pergamon Press, p.95 - 104

Wu C.Z., Gu W.B. and Hu Y.C., 1989, Coupled Heat Transfer of a Two-phase Closed Thermosyphon with Solidification. Proc. of 2nd Int. Symp. on Cold Regions Heat Transfer, p.183 - 188

Wu C. Z. and Gu W. B., 1993, Heat Transfer Prediction of Two-phase Closed Thermosyphon with Freezing, Proc. of 4th Int. Symp. on Cold Region Heat Transfer, p.219 - 297